

disordered topological quantum critical points in three-dimensional systems

Ryuichi Shindou

Condensed Matter Theory Laboratory, RIKEN, 2-1 Hirosawa, Wako, Saitama 351-0198, Japan

E-mail: rshindou@riken.jp

Ryota Nakai

Department of Physics, University of Tokyo, 7-3-1 Hongo, Bunkyo-ku, Tokyo 113-0033, Japan

Condensed Matter Theory Laboratory, RIKEN, 2-1 Hirosawa, Wako, Saitama 351-0198, Japan

E-mail: rnakai@riken.jp

Shuichi Murakami

Department of Physics, Tokyo Institute of Technology, 2-12-1 Ookayama, Meguro-ku, Tokyo 152-8551, Japan

PRESTO, Japan Science and Technology Agency 4-1-8 Honcho, Kawaguchi, Saitama 332-0012, Japan

E-mail: murakami@stat.phys.titech.ac.jp

Abstract. Generic non-magnetic disorder effects onto those topological quantum critical points (TQCP), which intervene the three-dimensional topological insulator and an ordinary insulator, are investigated. We first show that, in such 3-d TQCP, any backward scattering process mediated by the chemical-potential-type impurity is always canceled by its time-reversal (\mathcal{T} -reversal) counter-process, because of the non-trivial Berry phase supported by these two processes in the momentum space. However, this cancellation can be generalized into *only* those backward scattering processes which conserve a certain internal degree of freedom, i.e. the parity density, while the ‘absolute’ stability of the TQCP against *any* non-magnetic disorders is required by the bulk-edge correspondence. Motivated by this, we further derive the self-consistent-Born phase diagram in the presence of *generic* non-magnetic disorder potentials and argue the behaviour of the quantum conductivity correction in such cases. The distinction and similarity between the case with only the chemical-potential-type disorder and that with the generic non-magnetic disorders are finally summarized.

1. Why non-magnetic disorders in 3-d quantum spin Hall systems ?

A 3-d Z_2 quantum spin Hall insulator [1, 2, 3] is defined to be accompanied by the integer number of surface conducting channels, each of which is described by the 2+1 massless Dirac fermion, i.e. helical surface state. The stability of each helical surface state is protected by the Kramers degeneracy at the time-reversal (\mathcal{T} -) symmetric (surface) crystal momentum. The associated spin is directed within the XY plane, and rotates odd-number of times when the surface crystal momentum rotates once around this \mathcal{T} -symmetric k -point. While an individual helical surface state is protected by the \mathcal{T} -symmetry, level-crossings between any two different helical surface states are generally accidental: they can be lifted by a certain \mathcal{T} -symmetric perturbation [3, 4, 5, 6]. As a result of this pair annihilation, those insulators having even number of helical surface states can be adiabatically connected to an ordinary band insulator having no surface conducting channels at all ('weak topological insulator'). On the other hand, those with odd numbers of helical surface states are always accompanied by (at least) one gapless surface state, even when subjected under this pair annihilation ('strong topological insulator'). In the presence of the \mathcal{T} -symmetry, the latter type of insulators cannot be decomposed into any two copies of spinless wavefunctions, and therefore regarded as a new quantum state of matter which goes beyond the quantum Hall paradigm.

The quantum critical point [7, 8, 9, 10] which intervenes this 3-d topological insulator and a \mathcal{T} -symmetric ordinary band insulator is also non-trivial. That is, the stability of its critical nature is tightly connected to the stability of each helical surface state in the topological phase. To be specific, consider that a certain \mathcal{T} -symmetric model-parameter is changed, such that the system transits from the topological phase to a \mathcal{T} -symmetric ordinary phase. During this, the helical surface state in the topological phase is always protected by the \mathcal{T} -symmetry. When the system reaches the quantum critical point, however, the bulk-wavefunction becomes extended once. Thus, the two helical surface states localized at two opposite sample boundaries can communicate via this extended bulk-wavefunction, only to annihilate with each other. Thanks to this pair annihilation *mediated by the extended bulk*, the system can safely remove the stable helical surface state and enter the ordinary phase having no surface conducting channels, while simultaneously keeping the \mathcal{T} -symmetry. To put this reversely, the bulk-extended character of the quantum critical point is required to be stable against any \mathcal{T} -symmetric perturbations, provided that an individual helical surface state in the topological phase is stable against the same perturbations. Such a quantum critical point can be dubbed as the strong topological quantum critical point.

The above picture in the clean limit implies non-trivial disorder effects around this topological quantum critical point [11]. To describe this with clarity, let us first define three independently-tunable physical parameters in the topological phase: (i) the (topological) band gap W_{topo} , (ii) the band width of the conduction/valence band W_{band} , and (iii) non-magnetic disorder strengths W_{dis} . Provided that $W_{\text{dis}} < W_{\text{topo}}$, the helical surface state in the topological phase is stable against any non-magnetic disorders

irrespective of W_{band} [12, 13, 14]. On increasing W_{dis} such that $W_{\text{band}} < W_{\text{dis}} < W_{\text{topo}}$, those bulk-states far from the two band-centers, i.e. that of the conduction band and of the valence band, become localized (see Fig. 1(a)) [15]. Especially near the zero-energy region, $\mu = 0$, the system has no extended bulk wavefunctions. Thus, two helical surface states localized at the two opposite boundaries respectively are disconnected from each other. Starting from such a localized phase, consider decreasing the topological band gap (or increasing the disorder strength), such that $W_{\text{band}} < W_{\text{topo}} < W_{\text{dis}}$. During this decrease, these two disconnected surface states should communicate with each other once, so as to annihilate with each other, before the system enters the ordinary insulator phase. This requires that, at $W_{\text{topo}} \simeq W_{\text{dis}}$, the bulk-wavefunctions at $\mu \simeq 0$ must become extended once, so as to mediate these two opposite boundaries. Moreover, it also requires that such a bulk-extended region always intervenes between the topological phase and the ordinary insulator phase in the three-dimensional parameter space spanned by the chemical potential μ , W_{dis} and W_{topo} (see Fig. 1(b,c)). Such behaviour of the bulk extended region is often dubbed as the levitation and pair-annihilation phenomena, and was ubiquitously observed also in other topological systems, such as quantum Hall systems [16, 17, 18] and 2-d Z_2 quantum spin Hall systems [19, 20, 21].

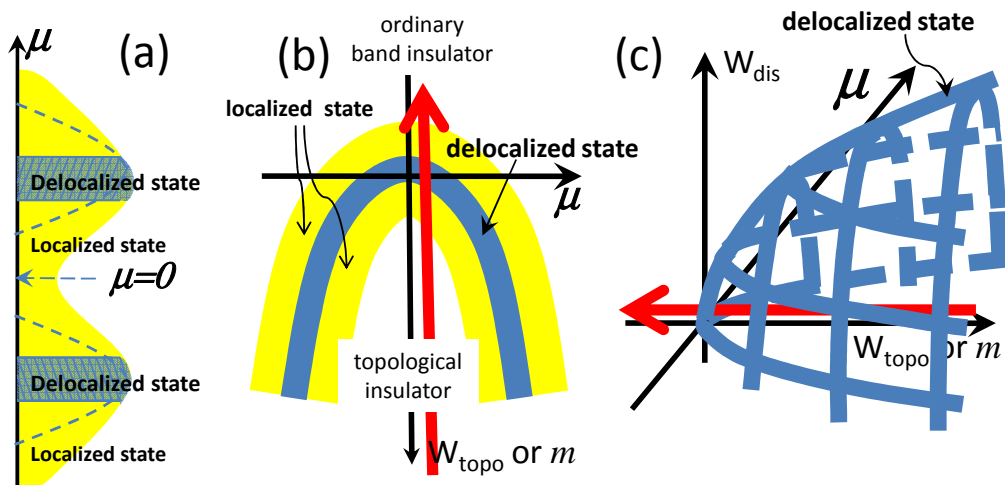


Figure 1. (a) A schematic density of state at $W_{\text{dis}} < W_{\text{topo}} (\equiv m)$. (b,c) schematic phase diagrams in the μ - W_{topo} - W_{dis} plane. The blue regions in these three figures stand for the delocalized state, which always intervenes between the topological insulator phase and an ordinary insulator phase in any ‘ \mathcal{T} -symmetric’ phase diagram. The figures are derived from Ref. [11].

Now that the 3-d Z_2 topological band insulator is a new quantum state of matter having no quantum-Hall analogue, the bulk-delocalized phase which intervenes this insulating phase (or localized state adiabatically connected to this) and the ordinary band insulator (or corresponding localized state) is also a new type of three-dimensional metallic phase, which has no analogue in any other condensed matter paradigms. Taking into account the chemical-potential type disorder (the most representative non-magnetic

disorder), we have previously studied [11] the self-consistent Born phase diagram around this topological metallic phase (or quantum critical point) and calculated the weak-localization correction to the charge conductivity. In actual solids [24, 25, 26, 27, 28], however, electronic disorders can generally exist not just in the chemical potential, but also in the transfer integral and spin-orbit interaction potential itself. On the one hand, the above argument based on the bulk-edge correspondence clearly dictates that the critical nature of the topological quantum critical point is stable against any of these non-magnetic disorders (not just against the chemical potential type disorder).

Motivated by this, we will treat in this paper various types of non-magnetic disorder potentials on an equal footing, so as to argue actual/generic properties of the topological quantum critical point in disordered Z_2 quantum spin Hall systems. The organization of this paper is as follows. In sec. 2, we summarize the effective continuum model studied in this paper. We next argue in sec. 3 that the non-trivial Berry phase (i.e. $e^{i\pi}$) inherent in the 3-d topological quantum critical point (TQCP) induces the perfect cancellation in the backward scattering channels mediated by the chemical-potential type disorder. This *partially* upholds the above argument based on the bulk-edge correspondence. However, it also becomes clear that this ‘Berry phase’ argument does *not necessarily* work in the presence of those non-magnetic disorders other than the chemical-potential type one. More accurately, those backward scattering processes which do not conserve a certain internal degree of freedom, i.e. parity density degree of freedom, are *not generally* set off by their \mathcal{T} -reversal counter processes. Promoted by this theoretical observation, we further derive in sec. 4 the self-consistent Born phase diagram in the presence of *generic* \mathcal{T} -symmetric disorder potentials. Based on this, we argue in sec. 5 the weak-localization correction to the charge conductivity in the presence of both the chemical-potential type disorder and the topological-mass type disorder. The distinctions between the case with only the chemical potential disorder and that with *generic* \mathcal{T} -symmetric disorders are summarized/clarified in sec. 6.

2. effective continuum model and \mathcal{T} -symmetric disorders

An effective continuum model describing the topological quantum critical point is given by a following 3 + 1 Dirac fermion [3, 7, 8, 9];

$$\mathcal{H}_0 \equiv \int d^3r \psi^\dagger(r) \left\{ \sum_{\mu=1}^3 \hat{\gamma}_\mu (-i\partial_\mu) + m\hat{\gamma}_5 \right\} \psi(r), \quad (1)$$

where the two massive phases, $m > 0$ and $m < 0$, represent the quantum spin Hall insulator and the \mathcal{T} -symmetric conventional (band) insulator respectively: ‘ m ’ corresponds to the topological band gap W_{topo} . The 4 by 4 γ -matrices consist of the Pauli spin matrix part \mathbf{s} and the other Pauli matrix $\boldsymbol{\sigma}$ representing the sublattice (or orbital) degree of freedom. There exist at most five such γ -matrices which anti-commute with one another. Here they are dubbed as $\gamma_1, \gamma_2, \gamma_3, \gamma_4$ and γ_5 . The product of these five always reduces to (the minus of) the unit matrix; $\hat{\gamma}_1\hat{\gamma}_2\hat{\gamma}_3\hat{\gamma}_4\hat{\gamma}_5 = -1$. Thus, even numbers

of γ -matrices out of these five should be time-reversal (\mathcal{T})-odd and spatial inversion (\mathcal{I})-odd. In eq. (1), three of them are already linearly coupled with the momentum. Thus, four of them should be both \mathcal{T} -odd and \mathcal{I} -odd. Without loss of generality, eq. (1) took $\gamma_{1,2,3,4}$ to be \mathcal{T} -odd and \mathcal{I} -odd, so that γ_5 is \mathcal{T} -even and \mathcal{I} -even. Under this convention, $\gamma_{15} \equiv -i\gamma_1\gamma_5$, γ_{25} , γ_{35} and γ_{45} are all \mathcal{T} -even and \mathcal{I} -odd, while γ_{12} , γ_{13} , γ_{14} , γ_{23} , γ_{34} and γ_{42} are all \mathcal{T} -odd and \mathcal{I} -even. Thus, arbitrary ‘on-site’ type non-magnetic disorder potentials are generally given by,

$$\mathcal{H}_{\text{imp}} \equiv \int d^3r \psi^\dagger(r) \left\{ v_0(r) \hat{\gamma}_0 + v_5(r) \hat{\gamma}_5 + \sum_{j=1}^4 v_{j5}(r) \hat{\gamma}_{j5} \right\} \psi(r). \quad (2)$$

with the real-valued functions v_j ($j = 0, 5, 15, \dots, 45$).

In Ref. [11], we have further assumed that the chemical-potential type disorders is the most dominant and have set the other five to be zero: $v_5 = v_{15} = \dots = v_{45} = 0$. Based on these simplifications, we have carried out the self-consistent Born analysis and weak-localization calculations, and obtained a simple microscopic picture, which can indeed explain how the bulk-extended region emerges when the topological band gap ‘ m ’ changes its sign [11]. In the next section, we will describe an alternative argument, which more directly dictates that the topological metallic phase (or quantum critical point) is free from any localization effect induced by generic non-magnetic disorders.

3. ‘Berry phase’ effect in 3-d topological metallic phases

Our argument here is a straightforward 3-dimensional generalization of the ‘Berry phase’ argument invented by Ando *et al.* [22] in the context of the carbon-nanotube (or 2-d graphene) subjected under *long*-range impurity potentials. Specifically, we will prove that an individual backward scattering process is precisely canceled by its time-reversal counterpart, which leads to a complete absence of the backward scattering in the 3-d topological quantum critical point.

Consider first the most simplest case, where the T -matrix is composed only by the chemical-potential-type impurity $v_0(r)$,

$$\hat{T} \equiv v_0 + v_0 \frac{1}{\epsilon - \hat{\gamma}_\mu(-i\partial_\mu)} v_0 + v_0 \frac{1}{\epsilon - \hat{\gamma}_\mu(-i\partial_\mu)} v_0 \frac{1}{\epsilon - \hat{\gamma}_\mu(-i\partial_\mu)} v_0 + \dots$$

In the momentum representation, the $(p+1)$ -th order backward scattering term reads,

$$\begin{aligned} \langle -k, \epsilon_{-k}, \sigma | \hat{T}^{(p+1)} | k, \epsilon_k, \sigma' \rangle &= \sum_{\tau_1, k_1, \sigma_1} \dots \sum_{\tau_p, k_p, \sigma_p} \frac{v_0(-k - k_p) \dots v_0(k_2 - k_1) v_0(k_1 - k)}{(\epsilon - \tau_p \epsilon_{k_p}) \dots (\epsilon - \tau_2 \epsilon_{k_2}) (\epsilon - \tau_1 \epsilon_{k_1})} \times \\ &\langle -k, \epsilon_{-k}, \sigma | k_p, \tau_p \epsilon_{k_p}, \sigma_p \rangle \times \dots \times \langle k_2, \tau_2 \epsilon_{k_2}, \sigma_2 | k_1, \tau_1 \epsilon_{k_1}, \sigma_1 \rangle \langle k_1, \tau_1 \epsilon_{k_1}, \sigma_1 | k, \epsilon_k, \sigma' \rangle, \quad (3) \end{aligned}$$

where $\tau_j = \pm$ ($j = 1, \dots, p$) in combination with ϵ_{k_j} specifies the eigen-energy of the hamiltonian at the momentum k_j , i.e. $\tau_j \epsilon_{k_j} = \pm |k_j|$. Such an eigen-energy is always accompanied by doubly degenerate eigen-states, which is specified by the spin index, $\sigma_j = \uparrow, \downarrow$. Namely, each eigen-state at the momentum k_j is uniquely identified by these two indices, $|k_j, \tau_j \epsilon_{k_j}, \sigma_j\rangle$. Without loss of generality, we can take the initial ket-state

and final bra-state to have an positive eigen-energy, i.e. $|k, \epsilon_k, \sigma\rangle$ and $\langle -k, \epsilon_{-k}, \sigma|$. We can also fix the gauge of the eigen-wavefunctions, e.g.

$$|k, \tau \epsilon_{k_j}, \sigma\rangle \equiv e^{i\frac{\theta}{2}(\sin \phi \hat{\gamma}_{23} - \cos \phi \hat{\gamma}_{31})} |\tau, \sigma\rangle_3 \equiv \hat{U}_k |\tau, \sigma\rangle_3,$$

with $k = |k|(\sin \theta \cos \phi, \sin \theta \sin \phi, \cos \theta)$. $|\tau, \sigma\rangle_3$ is the two-fold degenerate eigenstates of $\hat{\gamma}_3$ which belong to its eigenvalue τ , i.e. $\hat{\gamma}_3 |\tau, \sigma\rangle_3 \equiv \tau |\tau, \sigma\rangle_3$.

Based on this set-up, we can explicitly argue that the following two backward scattering processes, which are related by time-reversal operation, set off each other in eq. (3),

$$\begin{aligned} |k, +, \sigma\rangle &\rightarrow |k_1, \tau_1, \dots\rangle \rightarrow \dots \rightarrow |k_p, \tau_p, \dots\rangle \rightarrow |-k, +, \sigma'\rangle, \\ |k, +, \sigma\rangle &\rightarrow |-k_p, \tau_p, \dots\rangle \rightarrow \dots \rightarrow |-k_1, \tau_1, \dots\rangle \rightarrow |-k, +, \sigma'\rangle. \end{aligned}$$

where the summation over the spin indices associated with the intermediate states are assumed. To be more explicit, we can show that the following two have an opposite sign with each other,

$$\begin{aligned} S_{\sigma\sigma'}^{(p+1)} &= \sum_{\{\sigma_j\}} \langle -k, \epsilon_k, \sigma | k_p, \tau_p \epsilon_{k_p}, \sigma_p \rangle \dots \langle k_1, \tau_1 \epsilon_{k_1}, \sigma_1 | k, \epsilon_k, \sigma' \rangle, \\ S_{\sigma\sigma'}^{(p+1)'} &= \sum_{\{\sigma_j\}} \langle -k, \epsilon_k, \sigma | -k_1, \tau_1 \epsilon_{k_1}, \sigma_1 \rangle \dots \langle -k_p, \tau_p \epsilon_{k_p}, \sigma_p | k, \epsilon_k, \sigma' \rangle. \end{aligned}$$

for any σ and σ' . To see this, take the sum over all the intermediate spin indices first. This leads to

$$\begin{aligned} S_{\sigma\sigma'}^{(p+1)} &= {}_3\langle +, \sigma | \hat{U}_{-k}^\dagger \cdot (\hat{\gamma}_0 - n_{p,\mu} \hat{\gamma}_\mu) \dots (\hat{\gamma}_0 - n_{2,\nu} \hat{\gamma}_\nu) \cdot (\hat{\gamma}_0 - n_{1,\lambda} \hat{\gamma}_\lambda) \cdot \hat{U}_k | +, \sigma' \rangle_3, \\ S_{\sigma\sigma'}^{(p+1)'} &= {}_3\langle +, \sigma | \hat{U}_{-k}^\dagger \cdot (\hat{\gamma}_0 + n_{1,\mu} \hat{\gamma}_\mu) \cdot (\hat{\gamma}_0 + n_{2,\nu} \hat{\gamma}_\nu) \dots (\hat{\gamma}_0 + n_{p,\lambda} \hat{\gamma}_\lambda) \cdot \hat{U}_k | +, \sigma' \rangle_3. \end{aligned}$$

where n_j is a product between the normalized vector parallel to k_j and τ_j , $n_j \equiv \tau_j k_j / |k_j|$. The sequential product of the projection operators can be further expanded in this unit vector, i.e.

$$\begin{aligned} &(1 + n_p \cdot \gamma) \dots (1 + n_2 \cdot \gamma) \cdot (1 + n_1 \cdot \gamma) \\ &= 1 + \sum n_j \cdot \gamma + \sum_{i>j} (n_i \cdot \gamma)(n_j \cdot \gamma) + \dots + (n_p \cdot \gamma) \dots (n_2 \cdot \gamma)(n_1 \cdot \gamma). \end{aligned} \quad (4)$$

An even-order term in this expansion is always a linear combination of γ_0 , γ_{23} , γ_{31} and γ_{12} ,

$$(n_{2l} \cdot \gamma) \dots (n_1 \cdot \gamma) = A_l \gamma_0 + \epsilon_{\mu\nu\lambda} B_{l,\mu} \gamma_{\nu\lambda}.$$

A_l is a scalar quantity, which is composed only by inner products among $2l$ unit vectors. On the other hand, B_l clearly behaves as a vector, being coupled to γ_{23} , γ_{31} and γ_{12} . It is expressed as (a linear combination of) the product between $l-1$ inner products and one outer product,

$$B_{l,\mu} \equiv \sum_{l,m,\dots,n,o \neq i,j} b_{ij,lm\dots no}^l (n_i \times n_j)_\mu (n_l \cdot n_m) \dots (n_n \cdot n_o),$$

with some coefficients b_{\dots} free from $\{n_1, \dots, n_{2l}\}$. Multiply this even-order term by one additional $n \cdot \gamma$, one can obtain any odd-order term in eq. (4) as a linear combination of $\gamma_1, \gamma_2, \gamma_3$ and γ_{45} ;

$$(n_{2l+1} \cdot \gamma) \cdots (n_1 \cdot \gamma) = C_l \gamma_\mu + D_l \gamma_{45}.$$

C_l is a vector composed of l inner products, while D_l is a scalar containing one scalar triple product,

$$C_{l,\mu} = \sum_{n,o,\dots,p,q \neq m}^l c_{m,n,o,\dots,pq}^l n_{m,\mu} (n_n \cdot n_o) \cdots (n_p \cdot n_q),$$

$$D_l = \sum_{n,o,\dots,p,q \neq i,j,m}^l d_{ijm,n,o,\dots,pq}^l (n_i \times n_j) \cdot n_m (n_n \cdot n_o) \cdots (n_p \cdot n_q).$$

Thus, under the time-reversal operation, i.e. $(n_p, n_{p-1}, \dots, n_1) \rightarrow (-n_1, -n_2, \dots, -n_p)$, A_l and D_l do not change the sign, while B_l and C_l change their signs. These observations lead to a perfect cancellation between $S_{\sigma\sigma'}^{(p+1)}$ and $S_{\sigma\sigma'}^{(p+1)'}$,

$$\begin{aligned} S_{\sigma\sigma'}^{(p+1)} + S_{\sigma\sigma'}^{(p+1)'} &= 2 \sum_3 \langle +, \sigma | \hat{U}_{-k}^\dagger \cdot \{A\hat{\gamma}_0 + D\hat{\gamma}_{45}\} \cdot \hat{U}_k | +, \sigma' \rangle_3, \\ &= 2i \sum_3 \langle +, \sigma | (-\sin \phi \hat{\gamma}_{23} + \cos \phi \hat{\gamma}_{31}) \cdot (A\hat{\gamma}_0 + D\hat{\gamma}_{45}) | +, \sigma' \rangle_3 \\ &= \sum_{\sigma''} (\cdots) \cdot {}_3 \langle +, \sigma | -, \sigma'' \rangle_3 = 0, \end{aligned}$$

for arbitrary σ and σ' . This dictates that the backward-scattering process mediated by the chemical-potential-type disorder vanishes completely at the 3-d TQCP.

More generally, we can prove that any backward scattering process *which conserves the eigenvalue of $\hat{\gamma}_{45}$* is always set off by its corresponding \mathcal{T} -reversal counterpart. Such a process is always mediated by *even* number of either $v_{j5}(r)$ ($j = 1, 2, 3$) or $v_5(r)$, since both $\hat{\gamma}_{j5}$ ($j = 1, 2, 3$) and $\hat{\gamma}_5$ anticommute with $\hat{\gamma}_{45}$. To uphold the complete absence of the backward scattering in this case, we have only to show that the following two matrix elements have an opposite sign with each other,

$$\begin{aligned} S_{\sigma\sigma'}^{(p+1)} &= {}_3 \langle +, \sigma | \hat{U}_{-k}^\dagger \hat{\gamma}_{a_p} (\hat{\gamma}_0 - n_{p,\mu} \hat{\gamma}_\mu) \cdots \hat{\gamma}_{a_2} (\hat{\gamma}_0 - n_{2,\nu} \hat{\gamma}_\nu) \hat{\gamma}_{a_1} (\hat{\gamma}_0 - n_{1,\lambda} \hat{\gamma}_\lambda) \hat{\gamma}_{a_0} \hat{U}_k | +, \sigma' \rangle_3 \\ S_{\sigma\sigma'}^{(p+1)'} &= {}_3 \langle +, \sigma | \hat{U}_{-k}^\dagger \hat{\gamma}_{a_0} (\hat{\gamma}_0 + n_{1,\mu} \hat{\gamma}_\mu) \hat{\gamma}_{a_1} (\hat{\gamma}_0 + n_{2,\nu} \hat{\gamma}_\nu) \hat{\gamma}_{a_2} \cdots (\hat{\gamma}_0 + n_{p,\lambda} \hat{\gamma}_\lambda) \hat{\gamma}_{a_p} \hat{U}_k | +, \sigma' \rangle_3, \end{aligned}$$

for arbitrary σ and σ' . The indices a_0, a_1, a_2, \dots and a_p can be either 0, 15, 25, 35, 45 or 5, under the condition that the total number of those $\hat{\gamma}_{15}, \hat{\gamma}_{25}, \hat{\gamma}_{35}$ and $\hat{\gamma}_5$ which mediate the initial state and the final state is always *even*. To see the relative sign between these two, let us first transport all the intervening γ_{a_j} s in the leftward/rightward until they meet with the bra/ket states in $S_{\sigma\sigma'}^{(p+1)} / S_{\sigma\sigma'}^{(p+1)'}$. This transport brings about an appropriate redefinition of the normalized vectors, $n_j \rightarrow \bar{n}_j$,

$$\begin{aligned} S_{\sigma\sigma'}^{(p+1)} &= {}_3 \langle +, \sigma | \hat{U}_{-k}^\dagger \hat{\gamma}_{a_p} \cdots \hat{\gamma}_{a_1} \hat{\gamma}_{a_0} \cdot (\hat{\gamma}_0 - \bar{n}_{p,\mu} \hat{\gamma}_\mu) \cdots (\hat{\gamma}_0 - \bar{n}_{1,\lambda} \hat{\gamma}_\lambda) \hat{U}_k | +, \sigma' \rangle_3 \\ S_{\sigma\sigma'}^{(p+1)'} &= {}_3 \langle +, \sigma | \hat{U}_{-k}^\dagger (\hat{\gamma}_0 + \bar{n}_{1,\mu} \hat{\gamma}_\mu) \cdots (\hat{\gamma}_0 + \bar{n}_{p,\lambda} \hat{\gamma}_\lambda) \cdot \hat{\gamma}_{a_0} \hat{\gamma}_{a_1} \cdots \hat{\gamma}_{a_p} \hat{U}_k | +, \sigma' \rangle_3. \end{aligned}$$

$S^{(p+1)}$ and $S^{(p+1)'}$ is still connected by the \mathcal{T} -reversal operation, $(\bar{n}_p, \bar{n}_{p-1}, \dots, \bar{n}_1) \leftrightarrow (-\bar{n}_1, \dots, -\bar{n}_{p-1}, -\bar{n}_p)$. Thus, the preceding expansion can be used again,

$$\begin{aligned} (\hat{\gamma}_0 - \bar{n}_{p,\mu} \hat{\gamma}_\mu) \cdots (\hat{\gamma}_0 - \bar{n}_{2,\nu} \hat{\gamma}_\nu) (\hat{\gamma}_0 - \bar{n}_{1,\lambda} \hat{\gamma}_\lambda) &= \bar{A} \hat{\gamma}_0 + \bar{B}_\mu \epsilon_{\mu\nu\lambda} \hat{\gamma}_{\nu\lambda} + \bar{C}_\mu \hat{\gamma}_\mu + \bar{D} \hat{\gamma}_{45}, \\ (\hat{\gamma}_0 + \bar{n}_{1,\mu} \hat{\gamma}_\mu) (\hat{\gamma}_0 + \bar{n}_{2,\nu} \hat{\gamma}_\nu) \cdots (\hat{\gamma}_0 + \bar{n}_{p,\lambda} \hat{\gamma}_\lambda) &= \bar{A} \hat{\gamma}_0 - \bar{B}_\mu \epsilon_{\mu\nu\lambda} \hat{\gamma}_{\nu\lambda} - \bar{C}_\mu \hat{\gamma}_\mu + \bar{D} \hat{\gamma}_{45}. \end{aligned}$$

The condition imposed on a_j dictates that $\hat{\gamma}_{a_p} \cdots \hat{\gamma}_{a_1} \hat{\gamma}_{a_0}$ and $\hat{\gamma}_{a_0} \hat{\gamma}_{a_1} \cdots \hat{\gamma}_{a_p}$ always reduce to either (i) $\hat{\gamma}_j$ and $-\hat{\gamma}_j$ ($j = 1, 2, 3, 12, 23, 31$) respectively or (ii) $\hat{\gamma}_m$ and $\hat{\gamma}_m$ ($m = 0, 45$) respectively. Consider the former case first, e.g.

$$\begin{aligned} S_{\sigma\sigma'}^{(p+1)} &= {}_3\langle +, \sigma | \hat{U}_{-k}^\dagger \cdot \hat{\gamma}_1 \cdot (\bar{A}\hat{\gamma}_0 + \bar{B}\hat{\gamma}_{\nu\lambda} + \bar{C}\hat{\gamma}_\mu + \bar{D}\hat{\gamma}_{45}) \cdot \hat{U}_k | +, \sigma' \rangle_3 \\ &= {}_3\langle +, \sigma | \hat{U}_{-k}^\dagger \hat{U}_k \cdot m_\rho \hat{\gamma}_\rho \cdot (\bar{A}\hat{\gamma}_0 + \bar{B}'\hat{\gamma}_{\nu\lambda} + \bar{C}'\hat{\gamma}_\mu + \bar{D}\hat{\gamma}_{45}) | +, \sigma' \rangle_3, \\ S_{\sigma\sigma'}^{(p+1)'} &= {}_3\langle +, \sigma | \hat{U}_{-k}^\dagger \cdot (-\bar{A}\hat{\gamma}_0 + \bar{B}\hat{\gamma}_{\nu\lambda} + \bar{C}\hat{\gamma}_\mu - \bar{D}\hat{\gamma}_{45}) \cdot \hat{\gamma}_1 \cdot \hat{U}_k | +, \sigma' \rangle_3 \\ &= {}_3\langle +, \sigma | \hat{U}_{-k}^\dagger \hat{U}_k \cdot (-\bar{A}\hat{\gamma}_0 + \bar{B}'\hat{\gamma}_{\nu\lambda} + \bar{C}'\hat{\gamma}_\mu - \bar{D}\hat{\gamma}_{45}) \cdot m_\rho \hat{\gamma}_\rho | +, \sigma' \rangle_3. \end{aligned}$$

with $\hat{U}_{-k}^\dagger \hat{U}_k = -\sin\phi\hat{\gamma}_{23} + \cos\phi\hat{\gamma}_{31}$ and $m_\rho\hat{\gamma}_\rho \equiv \hat{U}_k^\dagger \hat{\gamma}_1 \hat{U}_k$. When $\hat{\gamma}_{a_p} \cdots \hat{\gamma}_{a_2} \hat{\gamma}_{a_1} = \hat{\gamma}_{12}$ (or $\hat{\gamma}_{23}, \hat{\gamma}_{31}$), $m_\rho\hat{\gamma}_\rho$ should be replaced by $m_\rho\epsilon_{\rho\phi\psi}\hat{\gamma}_{\phi\psi}$. In either cases, $S_{\sigma\sigma'}^{(p+1)}$ and $S_{\sigma\sigma'}^{(p+1)'}$ set off each other completely e.g.

$$\begin{aligned} \hat{S}_{\sigma\sigma'}^{(p+1)} + \hat{S}_{\sigma\sigma'}^{(p+1)'} &= {}_3\langle +, \sigma | (-s_\phi\gamma_{23} + c_\phi\gamma_{31}) \cdot \{\bar{B}'\hat{\gamma}_{\nu\lambda} + \bar{C}'\hat{\gamma}_\mu, m_\rho\hat{\gamma}_\rho\} | +, \sigma' \rangle_3 \\ &= 2 \times {}_3\langle +, \sigma | (-s_\phi\gamma_{23} + c_\phi\gamma_{31}) \cdot (\bar{B}'_m m_\mu \hat{\gamma}_{45} + \bar{C}'_\nu m_\nu \hat{\gamma}_0) | +, \sigma' \rangle_3 \\ &= (\cdots) \times {}_3\langle -, \sigma'' | +, \sigma' \rangle_3 = 0. \end{aligned}$$

A similar cancellation also holds true for the case with (ii) $\hat{\gamma}_{a_p} \cdots \hat{\gamma}_{a_2} \hat{\gamma}_{a_1} = \hat{\gamma}_{a_1} \hat{\gamma}_{a_2} \cdots \hat{\gamma}_{a_p} = \hat{\gamma}_{45}$. These observations thus conclude that any backward scattering process which conserves the eigenvalue of γ_{45} is always canceled by its time-reversal counter-process. Like in the 2-d graphene case [22], this cancellation is actually a direct consequence of the non-trivial Berry phase ' $e^{i\pi}$ ' accumulated along a closed loop composed by two time-reversal counterparts in the momentum space (see Fig. 2).

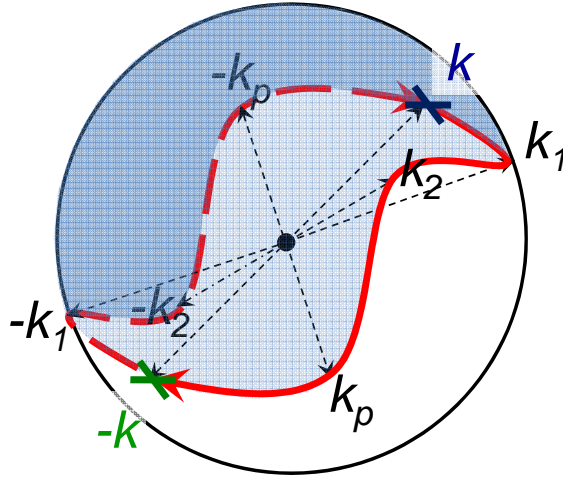


Figure 2. Red curves denote two backward scattering processes on a sphere in the momentum space ($|k_1| = \cdots = |k_p| = |k|$), which are mutually time-reversal to each other. The blue-shaded region, whose boundary is shaped by this two path, occupies *one half* of the whole surface of a sphere. Thus, an electron acquires the Berry phase π (instead of 2π), when it travels once around this boundary.

The above 'Berry phase' argument, however, does not hold true for the case with those backward scattering processes which change the eigenvalues of $\hat{\gamma}_{45}$. To see this,

consider, for example, the backward scattering processes mediated by *odd* number of $v_5(r)$ and compare following two \mathcal{T} -reversal paired processes,

$$\begin{aligned} S_{\sigma\sigma'}^{(p+1)} &= {}_3\langle +, \sigma | \hat{U}_{-k}^\dagger \cdot \hat{\gamma}_5 \cdot (\hat{\gamma}_0 - n_{p,\mu} \hat{\gamma}_\mu) \cdots (\hat{\gamma}_0 - n_{2,\nu} \hat{\gamma}_\nu) \cdot (\hat{\gamma}_0 - n_{1,\lambda} \hat{\gamma}_\lambda) \cdot \hat{U}_k | +, \sigma' \rangle_3, \\ S_{\sigma\sigma'}^{(p+1)'} &= {}_3\langle +, \sigma | \hat{U}_{-k}^\dagger \cdot (\hat{\gamma}_0 + n_{1,\mu} \hat{\gamma}_\mu) \cdot (\hat{\gamma}_0 + n_{2,\nu} \hat{\gamma}_\nu) \cdots (\hat{\gamma}_0 + n_{p,\lambda} \hat{\gamma}_\lambda) \cdot \hat{\gamma}_5 \cdot \hat{U}_k | +, \sigma' \rangle_3. \end{aligned}$$

We have already made any two ‘neighboring’ $\hat{\gamma}_5$ to annihilate each other, which leads an appropriate redefinition of the normalized unit vectors. The extra $\hat{\gamma}_5$ was then transported leftward/rightward in $S^{(p+1)}/S^{(p+1)'}$, until it meets with the bra/ket-state. Exploiting the expansion described above, we can readily see that these two do not cancel exactly in general,

$$S_{\sigma\sigma'}^{(p+1)} + S_{\sigma\sigma'}^{(p+1)'} = 2i \sum {}_3\langle +, \sigma | (-\sin \phi \hat{\gamma}_{23} + \cos \phi \hat{\gamma}_{31}) \cdot (A + \bar{C}_3 \hat{\gamma}_3) \cdot \hat{\gamma}_5 | +, \sigma' \rangle_3 \neq 0.$$

This situation is reminiscent of the 2-d graphene (or carbon-nanotube) subjected under *short-range* impurity potentials, where the *intervalley* scattering \ddagger suppresses the cancellation due to the Berry phase and consequently induces the crossover from the symplectic class to the orthogonal class [22, 23]. The situation in the 3-d TQCP is, however, quite different from this 2-d analogue. First of all, the preceding argument based on the bulk-edge correspondence requires the extended character of the 3-d TQCP to be stable against *any* non-magnetic disorders. Moreover, it always belongs to the symplectic class irrespectively of the type of non-magnetic disorders, which was not the case in the 2-d graphene [23]. Therefore, not only from the actual material’s viewpoint [24, 25, 26, 27, 28], but also from the theoretical standpoint, it is quite intriguing and important to investigate the effect of *general* \mathcal{T} -symmetric disorder potentials (including the topological-mass type one) in the 3-d topological metallic phase. In the next section, we will first study how a single-body Green function is renormalized by these *general* non-magnetic disorders. Based on this analysis, we will argue the behaviour of the quantum conductivity correction in the presence of both the chemical-potential type disorder v_0 and topological-mass type disorder v_5 .

4. self-consistent Born phase diagram – general case –

Consider $\mathcal{H}_0 + \mathcal{H}_{\text{imp}}$ with randomly distributed real-valued $v_j(r)$ ($j = 0, 5, \dots, 45$). Because of the \mathcal{T} -reversal symmetry, each eigenstate of this, say $|\psi_n(r)\rangle$, has its own Kramers-paired state $|\bar{\psi}_n(r)\rangle : \langle \bar{\psi}_n(r) | \equiv -i \hat{s}_y |\psi_n(r)\rangle$. Thus, the single-body Green functions obey the following relation;

$$\hat{G}^{R(A)}(r, r'; \mu) \equiv \sum_n \frac{|\psi_n(r)\rangle \langle \psi(r')|}{\mu - \epsilon_n \pm i\delta} = \hat{s}_y \{ \hat{G}^{R(A)}(r', r; \mu) \}^t \hat{s}_y, \quad (5)$$

where ‘+/-’ sign is for the retarded/advanced Green function $\hat{G}^{R/A}$.

\ddagger which corresponds to the *inter-’eigenvalue’* scattering in the current context.

The quenched disorder average is taken at the Gaussian level with the short-ranged correlation;

$$\overline{\cdots} \equiv \frac{1}{\mathcal{N}} \int \mathcal{D}[v] \cdots \exp \left[- \sum_{j,l} \int d^3r \Delta_{j,l} v_j(r) v_l(r) \right]. \quad (6)$$

Green functions thus averaged acquire the translational symmetry, $\hat{G}^{R(A)}(r, r'; \mu) = \hat{G}^{R(A)}(r - r'; \mu)$. When Fourier-transformed, they can be expanded in terms of the 16 γ -matrices with some complex-valued coefficients,

$$\hat{G}^R(k; \mu) = \sum_{n=1}^4 \hat{\gamma}_n \bar{F}_n(k; \mu) + \sum_{j=12,13,\dots}^{42} \hat{\gamma}_j \bar{F}_j(k; \mu) + \sum_{m=0,5} \hat{\gamma}_m \bar{F}_m(k; \mu) + \sum_{l=15}^{45} \hat{\gamma}_l \bar{F}_l(k; \mu),$$

and $\hat{G}^A(k; \mu) = \{\hat{G}^R(k; \mu)\}^\dagger$. The \mathcal{T} -symmetry requires $\bar{F}_{1,2,3,4}(k)$ and $\bar{F}_{12,13,14,23,34,42}(k)$ to be odd functions of k , while $\bar{F}_{0,5}(k)$ and $\bar{F}_{15,25,35,45}(k)$ to be even in k . Thus, only the latter six participate in the self-consistent Born equation,

$$\begin{aligned} \hat{\Sigma}^R(\mu) &\equiv \hat{G}_0^{R,-1}(k; \mu) - \hat{G}^{R,-1}(k; \mu) = \sum_{j,l} \Delta_{j,l} \int dk' \hat{\gamma}_j \cdot \hat{G}^R(k'; \mu) \cdot \hat{\gamma}_l, \\ &= \sum_{j,l} \Delta_{j,l} \int dk' \hat{\gamma}_j \cdot \left\{ \hat{\gamma}_0 \bar{F}_0(k') + \hat{\gamma}_5 \bar{F}_5(k') + \sum_{n=1}^4 \hat{\gamma}_{n5} \bar{F}_{n5}(k') \right\} \cdot \hat{\gamma}_l. \end{aligned} \quad (7)$$

The bare Green function is defined as,

$$\hat{G}_0^{R,-1}(k; \mu) = (\mu + i\delta) \hat{\gamma}_0 - \sum_{j=1}^3 k_j \hat{\gamma}_j - m \hat{\gamma}_5 \equiv \sum_{j=0,1,\dots,5} \mathbf{f}_j \hat{\gamma}_j.$$

The inverse of the Green function thus determined is at most a linear combination of γ_0 , γ_5 , γ_{15} , \dots and γ_{45} ,

$$G^{R,-1}(\mu) \equiv F_0 \hat{\gamma}_0 + F_5 \hat{\gamma}_5 + \sum_{j=1}^4 F_{j5} \hat{\gamma}_{j5}.$$

Eq. (7) determines their coefficients,

$$\begin{aligned} F_0 - \mathbf{f}_0 &= - \left\{ \Delta_{0,0} + \Delta_{5,5} + \sum_{j=1}^4 \Delta_{j5,j5} \right\} \cdot \int d^3k' \bar{F}_0(k') \\ &\quad - 2\Delta_{0,5} \int d^3k' \bar{F}_5(k') - 2 \sum_{j=1}^4 \left\{ \Delta_{0,j5} \int d^3k' \bar{F}_{j5}(k') \right\}, \end{aligned} \quad (8)$$

$$\begin{aligned} F_5 - \mathbf{f}_5 &= - \left\{ \Delta_{0,0} + \Delta_{5,5} - \sum_{j=1}^4 \Delta_{j5,j5} \right\} \cdot \int d^3k' \bar{F}_5(k') \\ &\quad - 2\Delta_{0,5} \int d^3k' \bar{F}_0(k') - 2 \sum_{j=1}^4 \left\{ \Delta_{5,j5} \int d^3k' \bar{F}_{j5}(k') \right\}, \end{aligned} \quad (9)$$

$$F_{j5} = - \left\{ \Delta_{0,0} - \Delta_{5,5} - \sum_{m=1}^4 \Delta_{m5,m5} \right\} \cdot \int d^3k' \bar{F}_{j5}(k')$$

$$-2\Delta_{0,j5} \int d^3k' \bar{F}_0(k') - 2\Delta_{5,j5} \int d^3k' \bar{F}_5(k') - 2 \sum_{m=1}^4 \left\{ \Delta_{m5,j5} \int d^3k' \bar{F}_{m5}(k') \right\}. \quad (10)$$

That is, the right hand sides are given by these coefficients themselves,

$$\begin{aligned} \bar{F}_0(k) &= -\frac{F_0}{g(k)} \left\{ k^2 - F_0^2 + F_5^2 + \sum_{j=1}^4 F_{j5}^2 \right\}, & \bar{F}_5(k) &= \frac{F_5}{g(k)} \left\{ k^2 - F_0^2 + F_5^2 + \sum_{j=1}^4 F_{j5}^2 \right\}, \\ \bar{F}_{j5}(k) &= -\frac{F_{j5}}{g(k)} \left\{ k^2 + F_0^2 - F_5^2 - \sum_{m=1}^4 F_{m5}^2 \right\} - (1 - \delta_{j4}) \frac{2k_j}{g(k)} \left\{ \sum_{m=1}^3 F_{m5} k_m \right\}, \end{aligned}$$

with $g(k)$ being defined as,

$$g(k) \equiv \left\{ -F_0^2 + F_5^2 + \sum_{j=1}^4 F_{j5}^2 - k^2 \right\}^2 + 4k^2 \left\{ F_5^2 - F_0^2 \right\} + 4 \left\{ \sum_{m=1}^3 F_{m5} k_m \right\}^2.$$

Note that all integrals in eqs. (8,9) depend on the ultraviolet cutoff; $\int d^3k \equiv \int_{|k| < \Lambda} d^3k$.

We will solve these coupled integral equations, assuming that *the spatial inversion symmetry is recovered after the quenched average*. Namely, we assume

$$\hat{\gamma}_5 \cdot \hat{G}^{R(A)}(k; \mu) \cdot \hat{\gamma}_5 = \hat{G}^{R(A)}(-k; \mu), \quad (11)$$

because only γ_5 anticommutes with both $\gamma_{1,\dots,4}$ and $\gamma_{15,\dots,45}$. This requires $\Delta_{0,j5}$, $\Delta_{5,j5}$ and F_{j5} ($j = 1, \dots, 4$) to be zero, so that the equation becomes,

$$\begin{bmatrix} F_0 \\ F_5 \end{bmatrix} + G \begin{bmatrix} \Delta_s + \Delta_a & -B \\ B & -\Delta_s + \Delta_a \end{bmatrix} \begin{bmatrix} F_0 \\ F_5 \end{bmatrix} = \begin{bmatrix} \mu \\ -m \end{bmatrix}, \quad G = 2 \int_0^1 \frac{k^2 dk}{F_0^2 - F_5^2 - k^2} \quad (12)$$

with $\Delta_s \equiv 2\pi\Lambda(\Delta_{0,0} + \Delta_{5,5})$, $\Delta_a \equiv \sum_{j=1}^5 2\pi\Lambda\Delta_{j5,j5}$, and $B = 4\pi\Lambda\Delta_{0,5}$. In eq. (12), the momenta and energies are rescaled by the ultraviolet cut-off Λ ,

$$\Lambda \rightarrow 1, \quad k \rightarrow k\Lambda^{-1}, \quad F_{0,5} \rightarrow F_{0,5} \equiv F_{0,5}\Lambda^{-1}, \quad (\mu, m)_{\text{old}} \rightarrow (\mu, m)_{\text{new}} \equiv (\mu, m)_{\text{old}}\Lambda^{-1}. \quad (13)$$

The first part of eq. (12) can be ‘diagonalized’ by the following canonical transformation,

$$\begin{bmatrix} \mathcal{F}_0 \\ \mathcal{F}_5 \end{bmatrix} = \begin{bmatrix} \text{ch}\theta & -\text{sh}\theta \\ -\text{sh}\theta & \text{ch}\theta \end{bmatrix} \begin{bmatrix} F_0 \\ F_5 \end{bmatrix}, \quad \begin{bmatrix} \psi_1 \\ \psi_2 \end{bmatrix} = \begin{bmatrix} \text{ch}\theta & -\text{sh}\theta \\ -\text{sh}\theta & \text{ch}\theta \end{bmatrix} \begin{bmatrix} \mu \\ -m \end{bmatrix}, \quad (14)$$

where the angle θ is chosen as

$$(\text{ch}\theta, \text{sh}\theta) \equiv \frac{(\Delta_s + \sqrt{\Delta_s^2 - B^2}, B)}{\sqrt{2}\{\Delta_s^2 - B^2\}^{\frac{1}{4}}\{\sqrt{\Delta_s^2 - B^2} + \Delta_s\}^{\frac{1}{2}}}. \quad (15)$$

Under this transformation, we obtain,

$$\begin{cases} (1 + \eta_+ G)\mathcal{F}_0 = \psi_1 \\ (1 - \eta_- G)\mathcal{F}_5 = \psi_2, \end{cases} \quad G = 2 \int_0^1 \frac{k^2 dk}{\mathcal{F}_0^2 - \mathcal{F}_5^2 - k^2} \equiv 2 \int_0^1 \frac{k^2 dk}{(a + ib)^2 - k^2}, \quad (16)$$

with $\eta_{\pm} = \sqrt{\Delta_s^2 - B^2} \pm \Delta_a$ and $(a + ib)^2 \equiv \mathcal{F}_0^2 - \mathcal{F}_5^2$. The real/imaginary part of ‘ G ’ is an even/odd function of both a and b ,

$$\text{Re}G = -2 - \frac{a}{2} \log \left[\frac{(1-a)^2 + b^2}{(1+a)^2 + b^2} \right] + b \left(\arctan \left[\frac{1-a}{b} \right] + \arctan \left[\frac{1+a}{b} \right] \right), \quad (17)$$

$$\text{Im}G = -\frac{b}{2} \log \left[\frac{(1-a)^2 + b^2}{(1+a)^2 + b^2} \right] - a \left(\arctan \left[\frac{1-a}{b} \right] + \arctan \left[\frac{1+a}{b} \right] \right). \quad (18)$$

Eqs. (16-18) can be solved in a quite similar fashion as we did in Ref [11] (compare them with eqs. (38-41) in this reference). As a result, the final self-consistent Born phase diagram obtained in this section is basically same as that obtained there. The only difference is that the phase boundaries which separate two gapped phases and compressible (diffusive) phase are deformed in the μ - m parameter space, according to the canonical transformation eq. (14): they become symmetric with respect to ψ_1 and ψ_2 , instead of μ and m (compare Fig. 5 with Figs. 9,10 in the reference). Those who are well-informed of Ref. [11] therefore might as well skip the remaining part of this section and start from sec. 5. To make this article self-contained, we will review the arguments in the context of eqs. (16-18).

4.1. $\psi_1 = \psi_2 = 0$ case

Consider the simplest case first, $\mu = m = 0$. Since $\eta_+ + \eta_- \equiv 2\sqrt{\Delta_s^2 - B^2} \neq 0$ §, the possible solutions of eqs. (16-18) are clearly three-folded:

$$\begin{cases} \text{(i)} : \mathcal{F}_0 = \mathcal{F}_5 = 0, \\ \text{(ii)} : 1 + \eta_+ G = 0 \cap \mathcal{F}_5 = 0, \\ \text{(iii)} : 1 - \eta_- G = 0 \cap \mathcal{F}_0 = 0. \end{cases} \quad (19)$$

The type-(iii) solution can realize when $\eta_- < -\frac{1}{2}$. In reality, however, such a parameter region is very limited and the solution itself is also physically unlikely. Thus, we will investigate only the first two types.

The type-(i) solution is a diffusionless solution, where the massless zero-energy state is free from any disorders. The type-(ii) solution describes the diffusive massless state: the zero energy state at the critical point acquires a finite life-time due to the non-magnetic disorders. The gap equations have an intrinsic critical disorder strength $\eta_{+,c}$, below which only the type-(i) solution is allowed. When the disorder strength exceeds this critical value, $\eta_+ > \eta_{+,c}$, this type-(i) solution becomes unphysical and type-(ii) solution becomes a unique physical solution. These two solutions are continuously connected at $\eta_+ = \eta_{+,c}$.

To see this situation, begin with the type-(ii) solution:

$$1 + \eta_+ \text{Re}G = 0 \cap \text{Im}G = 0 \cap \mathcal{F}_5 = 0. \quad (20)$$

$\text{Im}G = 0$ requires either (a) $a = 0$ or (b) $b = 0 \cap |a| > 1$. Now that ‘ a ’ and ‘ b ’ as well as ‘ F_0 ’ and ‘ F_5 ’ are rescaled by the ultraviolet cutoff Λ as in eq. (13), they should be much smaller than unit. This leads to $a = 0$. With this, $1 + \eta_+ \text{Re}G = 0$ determines ‘ b ’ as a function of the disorder strength η_+ :

$$b \cdot \arctan[b^{-1}] = 1 - \frac{1}{2\eta_+}. \quad (21)$$

This equation dictates that ‘ b ’ can be finite only when η_+ is greater than some critical value. That is $\eta_{+,c} = \frac{1}{2}$. Above this, the type-(ii) solution becomes possible,

§ The convergence of the gaussian integral in eq. (6) requires $\Delta_s > B$.

$(\mathcal{F}_0, \mathcal{F}_5) = (ib, 0)$. When the disorder strength falls below this critical value, the solution reduces continuously to the trivial one, $(\mathcal{F}_0, \mathcal{F}_5) = (0, 0)$. In the followings, we will summarize the behaviours of these two solutions in the presence of finite ψ_1 and ψ_2 .

4.2. $\psi_1 \neq 0$ and $\psi_2 = 0$ case

Introduce small ψ_1 into the type-(i) solution first. Employing $\mathcal{F}_5 = 0$, we have only to solve the first line of eq. (16) in favor for $a + ib = \mathcal{F}_0$. Since its real part, \mathcal{F}'_0 , is an odd function of ψ_1 and its imaginary part \mathcal{F}''_0 is even in ψ_1 , ‘ a ’ is the first order in small ψ_1 while ‘ b ’ is the second order, $a = \mathcal{O}(\psi_1)$ and $b = \mathcal{O}(\psi_1^2)$. With this, eq. (16) can be solved iteratively in small ψ_1 :

$$a = \frac{\psi_1}{1 - 2\eta_+} + \mathcal{O}(\psi_1^3), \quad b = \frac{\pi\eta_+}{(1 - 2\eta_+)^3} \psi_1^2 + \mathcal{O}(\psi_1^4). \quad (22)$$

This indicates that, for $\eta_+ > \eta_{+,c}$, the sign of the renormalized chemical potential ‘ a ’ and that of the bare chemical potential ‘ ψ_1 ’ becomes opposite with each other. This is, however, physically unlikely. When η_+ exceeds this critical strength, the type-(ii) solution instead of type-(i) becomes a physical solution. Indeed, having a finite ‘ b ’ already at the zero-th order in ψ_1 , the type-(ii) solution behaves as follows,

$$a = \frac{\psi_1}{2\eta_+ - 1} + \mathcal{O}(\psi_1^3, b^2\psi_1), \quad b = \frac{1}{\pi} \frac{2\eta_+ - 1}{\eta_+} + \mathcal{O}(\psi_1^2, b^2), \quad (23)$$

in small ψ_1 region. For $\eta_+ > \eta_{+,c}$, ‘ a ’ has the same sign as that of the bare one.

4.3. $\psi_1 = 0$ and $\psi_2 \neq 0$ case

In the presence of finite ψ_2 , the solutions of eqs. (16-18) are two-folded, depending on the relative ratio between the disorder strength and the topological mass ψ_2 . When the topological mass is less than a certain critical value, say $\psi_{2,c}$, the system is in the diffusive (compressible) phase, which is basically equivalent to the type-(ii) solution at $\psi_2 = 0$,

$$\mathcal{F}_0 = i\sqrt{\tau^{-2} - \left(\frac{\eta_+\psi_2}{\eta_+ + \eta_-}\right)^2}, \quad \mathcal{F}_5 = \frac{\eta_+\psi_2}{\eta_+ + \eta_-}. \quad (24)$$

τ^{-1} and $\psi_{2,c}$ are defined by η_{\pm} :

$$\psi_{2,c}(\eta_+, \eta_-) = \frac{\eta_+ + \eta_-}{\eta_+ \tau}, \quad \tau^{-1} \arctan[\tau] = 1 - \frac{1}{2\eta_+}. \quad (25)$$

When ψ_2 exceeds this critical value, the system enters one of the two incompressible phases, which is adiabatically connected to the gapped phases in the clean limit,

$$\mathcal{F}_0 = 0, \quad \mathcal{F}_5 = \bar{\psi}_2. \quad (26)$$

The renormalized mass terms $\bar{\psi}_2$ is given by

$$\bar{\psi}_2 \{1 + 2\eta_- - 2\eta_- \bar{\psi}_2 \arctan[\bar{\gamma}_2^{-1}]\} = \psi_2. \quad (27)$$

These two solutions are connected continuously at the phase boundary, $\psi_2 = \psi_{2,c}(\eta_+, \eta_-)$.

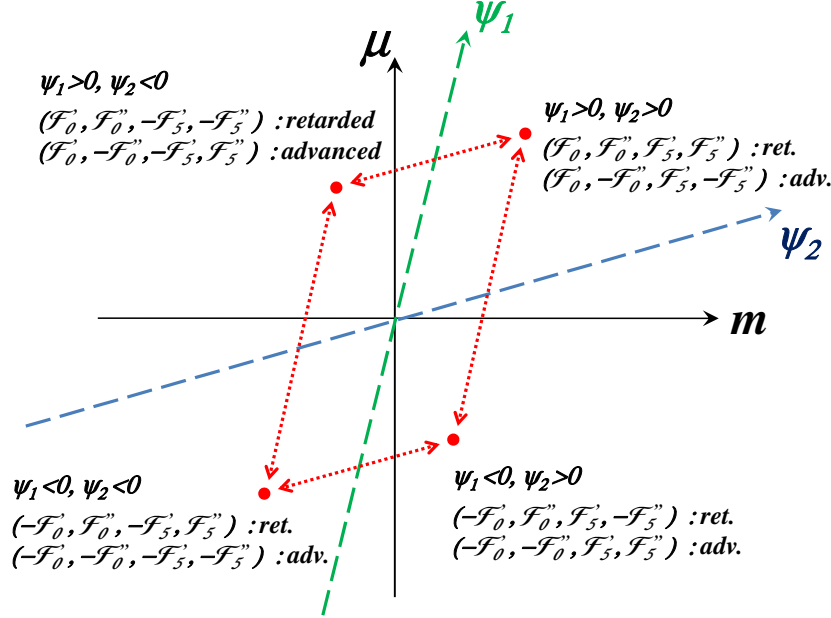
4.4. $\psi_1 \neq 0$ and $\psi_2 \neq 0$ case


Figure 3. $\mathcal{F}_0 = \mathcal{F}_0' + i\mathcal{F}_0''$ and $\mathcal{F}_5 = \mathcal{F}_5' + i\mathcal{F}_5''$ as a function of bare chemical potential μ and topological mass m . \mathcal{F}_0 changes its sign under $\psi_1 \rightarrow -\psi_1$, while \mathcal{F}_5 changes its sign under $\psi_2 \rightarrow -\psi_2$.

For general ψ_1 and ψ_2 , we have solved numerically the following coupled equations in favor of ‘a’ and ‘b’:

$$\mathcal{F}_0 = \frac{\psi_1(1 + \eta_+ \text{Re}G)}{(1 + \eta_+ \text{Re}G)^2 + (\eta_+ \text{Im}G)^2} + i \frac{\psi_1 \eta_+ \text{Im}G}{(1 + \eta_+ \text{Re}G)^2 + (\eta_+ \text{Im}G)^2},$$

$$\mathcal{F}_5 = \frac{\psi_2(1 + \eta_- \text{Re}G)}{(1 + \eta_- \text{Re}G)^2 + (\eta_- \text{Im}G)^2} + i \frac{\psi_2 \eta_- \text{Im}G}{(1 + \eta_- \text{Re}G)^2 + (\eta_- \text{Im}G)^2},$$

with $\mathcal{F}_0^2 - \mathcal{F}_5^2 = (a + ib)^2$ and $\text{Re}G$ and $\text{Im}G$ defined in eqs. (17,18). The numerical solutions thus obtained are clearly four-folded, i.e. (a, b) , $(-a, b)$, $(a, -b)$ and $(-a, -b)$. This leads to double degeneracy in \mathcal{F}_0 and \mathcal{F}_5

$$(\mathcal{F}_0', \mathcal{F}_0'', \mathcal{F}_5', \mathcal{F}_5''), (\mathcal{F}_0', -\mathcal{F}_0'', \mathcal{F}_5', -\mathcal{F}_5''),$$

with $\mathcal{F}_0 \equiv \mathcal{F}_0' + i\mathcal{F}_0''$ and $\mathcal{F}_5 \equiv \mathcal{F}_5' + i\mathcal{F}_5''$. Moreover, these two solutions at (ψ_1, ψ_2) are related to those at the other three points, i.e. $(\psi_1, -\psi_2)$, $(-\psi_1, \psi_2)$ and $(-\psi_1, -\psi_2)$,

$$\begin{aligned} (\mathcal{F}_0', \pm \mathcal{F}_0'', \mathcal{F}_5', \pm \mathcal{F}_5'')|_{\psi_1, \psi_2} &= (\mathcal{F}_0', \pm \mathcal{F}_0'', -\mathcal{F}_5', \mp \mathcal{F}_5'')|_{\psi_1, -\psi_2} \\ &= (-\mathcal{F}_0', \pm \mathcal{F}_0'', \mathcal{F}_5', \mp \mathcal{F}_5'')|_{-\psi_1, \psi_2} = (-\mathcal{F}_0', \pm \mathcal{F}_0'', -\mathcal{F}_5', \pm \mathcal{F}_5'')|_{-\psi_1, -\psi_2}. \end{aligned} \quad (28)$$

The upper/lower sign is for the retarded/advanced Green function (Fig. 3).

Fig. 4 demonstrates how \mathcal{F}_0 and \mathcal{F}_5 behave as a function of μ and m , both for $\eta_+ < \eta_{+,c}$ and for $\eta_+ > \eta_{+,c}$. Fig. 5 is the corresponding phase diagrams, where both \mathcal{F}_0'' and \mathcal{F}_5'' vanish in two incompressible phases (the topological insulator and

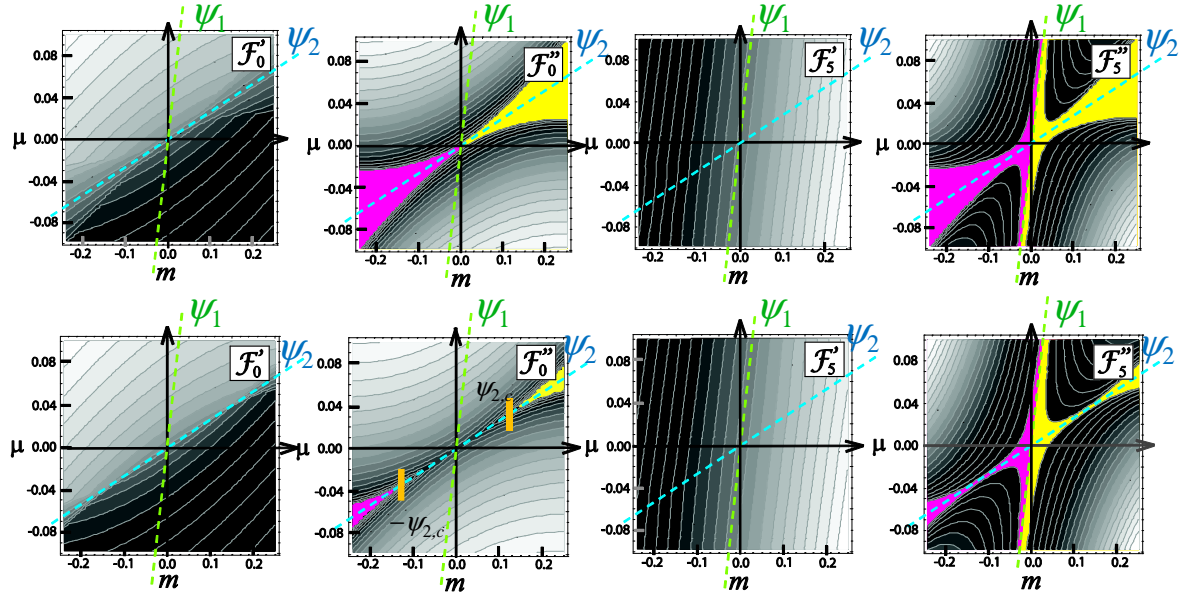


Figure 4. $(\mathcal{F}_0, \mathcal{F}_5)$ numerically evaluated at $\Delta_a/\Delta_s = B/\Delta_s = 0.5$ and $\eta_+ = 0.45/0.57$ (upper/lower four panels). Their real parts and imaginary parts decrease/increase toward the dark/light region. (upper/lower four from left to right): The contour plot of \mathcal{F}_0' , \mathcal{F}_0'' , \mathcal{F}_5' and \mathcal{F}_5'' at $\eta_+ = 0.45/0.57$. The contour intervals are $0.32/0.30 \times 10^{-1}$, $0.9/1.25 \times 10^{-2}$, $0.24/0.24 \times 10^{-1}$ and $0.68/0.75 \times 10^{-3}$ respectively. Both \mathcal{F}_0' and \mathcal{F}_5'' become zero at $\psi_1 = 0$. \mathcal{F}_0'' and \mathcal{F}_5' vanish within both the yellow region (topological insulator) and the red region (ordinary insulator). \mathcal{F}_0'' in the lower panel remains finite even at $\psi_1 = 0$, as far as $-\psi_{2,c} < \psi_2 < \psi_{2,c}$, where $\psi_{2,c}$ is given by eq. (25).

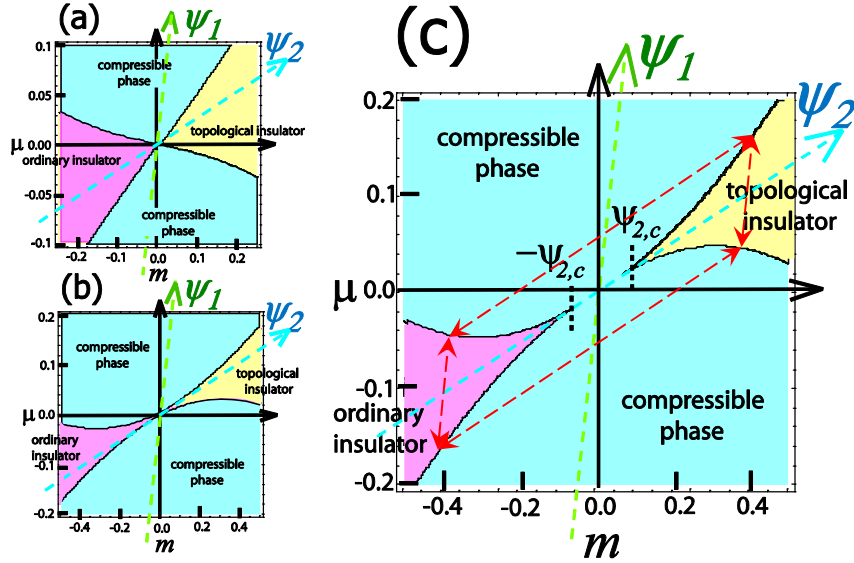


Figure 5. The self-consistent Born phase diagram for fixed $\Delta_a/\Delta_s = B/\Delta_s = 0.5$. (a/b/c) $\eta_+ = 0.31/0.48/0.53$, where $\eta_{+,c} = 0.5$.

an ordinary insulator). For $\eta_+ < \eta_{+,c}$, the μ - m phase diagram holds a *direct* phase transition point between these two gapped phases (Fig. 5(a,b)). For $\eta_+ > \eta_{+,c}$, this direct phase transition point becomes a *finite region* of the diffusive phase (Fig. 5(c)). Especially at $\psi_1 = 0$, this diffusive region ranges from $\psi_2 = -\psi_{2,c}$ to $\psi_2 = \psi_{2,c}$, where $\psi_{2,c}$ is given by eq. (25). Note also that, due to the symmetry relation given in eq. (28), all the phase boundaries are symmetric with respect to the sign changes of ψ_1 and ψ_2 (see red arrows in Fig. 5(c)).

5. quantum conductivity correction in the presence of the topological-mass type disorder potential

We will argue the behaviour of the quantum conductivity correction in the presence of both chemical-potential type disorder and topological-mass type disorder. To do this, consider the following series-sum of the ladder type diagrams;

$$\Gamma^{\text{dif}}(q, \omega) = \left[\hat{\xi}^{-1} - \sum_k \hat{G}^R(k_+, \mu_+) \times \hat{G}^A(k_-, \mu_-) \right]^{-1} \quad (29)$$

where $k_{\pm} \equiv k \pm \frac{q}{2}$, $\mu_{\pm} \equiv \mu \pm \frac{\omega}{2}$ and the 16 by 16 tensor $\hat{\xi}$ is given by ||;

$$\hat{\xi} \equiv \Delta_{0,0} \hat{\gamma}_0 \times \hat{\gamma}_0 + \Delta_{0,5} \hat{\gamma}_5 \times \hat{\gamma}_0 + \Delta_{5,0} \hat{\gamma}_0 \times \hat{\gamma}_5 + \Delta_{5,5} \hat{\gamma}_5 \times \hat{\gamma}_5.$$

Tracing out its two vertices with some internal degree of freedom, say $\hat{\gamma}_j$, we obtain the correlation function of the corresponding density $\psi^\dagger \hat{\gamma}_j \psi$,

$$\begin{aligned} \phi_j(q, \omega) \equiv & -\frac{1}{2\pi i} \sum_{\alpha, \dots, \theta} \sum_{k, k'} [\hat{\gamma}_j]_{\beta\alpha} \hat{G}_{\alpha\epsilon}^R(k_+, \mu_+) \hat{G}_{\zeta\beta}^A(k_-, \mu_-) \\ & \{ \delta_{k,k'} \delta_{\epsilon\delta} \delta_{\gamma\zeta} + \Gamma_{\epsilon\theta, \eta\zeta}^{\text{dif}}(q, \omega) \hat{G}_{\theta\delta}^R(k'_+, \mu'_+) \hat{G}_{\gamma\eta}^A(k'_-, \mu'_-) \} [\hat{\gamma}_j]_{\delta\gamma} \end{aligned} \quad (30)$$

When this density is a conserved quantity in each ensemble, like $\psi^\dagger \hat{\gamma}_0 \psi$, the function should exhibit the diffusive behaviour at the infrared region, $q, \omega \simeq 0$. Thus, the above series-sum carries at least one diffusion pole. When its advanced line is \mathcal{T} -reversed, it is transcribed into the series-sum of the ‘maximally-crossed’ diagrams (Cooperon),

$$\begin{aligned} (1 \otimes s_y)_{\gamma\gamma'} \Gamma_{\alpha\delta, \beta'\gamma'}^{\text{dif}}(q, \omega) (1 \otimes s_y)_{\beta'\beta} = & \sum_{i,j=0,5} \Delta_{i,j} [\hat{\gamma}_i]_{\alpha\delta} \times [\hat{\gamma}_j]_{\gamma\beta} \\ + \sum_{i, \dots, m} \sum_k \Delta_{i,j} \Delta_{l,m} [\hat{\gamma}_i]_{\alpha\alpha_1} \hat{G}_{\alpha_1\delta_1}^R(k_+, \mu_+) [\hat{\gamma}_l]_{\delta_1\delta} \times & [\hat{\gamma}_j]_{\gamma\gamma_1} \hat{G}_{\gamma_1\beta_1}^A(-k_-, \mu_-) [\hat{\gamma}_m]_{\beta_1\beta} \\ + \sum_{i, \dots, p} \sum_{k, k'} \Delta_{i,j} \Delta_{l,m} \Delta_{n,p} [\hat{\gamma}_i]_{\alpha\alpha_1} \hat{G}_{\alpha_1\delta_1}^R(k_+, \mu_+) [\hat{\gamma}_l]_{\delta_1\alpha_2} \hat{G}_{\alpha_2\delta_2}^R(k'_+, \mu'_+) & [\hat{\gamma}_n]_{\delta_2\delta} \\ \times [\hat{\gamma}_j]_{\gamma\gamma_1} \hat{G}_{\gamma_1\beta_1}^A(-k_-, \mu_-) [\hat{\gamma}_m]_{\beta_1\gamma_2} \hat{G}_{\gamma_2\beta_2}^A(-k'_-, \mu'_-) [\hat{\gamma}_p]_{\beta_2\beta} + \dots, \end{aligned} \quad (31)$$

which describes the quantum interference between the time-reversal paired scattering process from K to $-K + q$. Thus, any type of the diffusion pole appearing in eq. (29)

|| Note that the product between these tensors is defined as $(\hat{A}_r \times \hat{A}_a) \cdot (\hat{B}_r \times \hat{B}_a) \equiv \hat{A}_r \hat{B}_r \times \hat{B}_a \hat{A}_a$, where \hat{A}_r (\hat{B}_r) is a 4 by 4 matrix in the retarded line, while \hat{A}_a (\hat{B}_a) stands for that in the advanced line.

generally results in a certain quantum interference effect in the backward scattering channel.

To investigate the nature of the diffusion poles in eq. (29), employ the canonical transformation used in sec. 4 first,

$$\begin{aligned}\bar{\Gamma}^{\text{dif}}(q, \omega) &\equiv V_\theta^R \times V_\theta^A \cdot \Gamma^{\text{dif}}(q, \omega) \cdot V_\theta^R \times V_\theta^A, \\ V_\theta^R &= V_\theta^A = \cosh \frac{\theta}{2} \hat{\gamma}_0 + \sinh \frac{\theta}{2} \hat{\gamma}_5,\end{aligned}$$

with θ being defined as eq. (15). Such a transformation diagonalizes $\hat{\xi}$. Simultaneously, it simplifies the expression of $\hat{G}^{R(A)}(k_\pm, \mu_\pm)$ in terms of \mathcal{F}_0 and \mathcal{F}_5 . Namely, the series-sum thus transformed reads

$$\bar{\Gamma}^{\text{dif}}(q, \omega) = \left[\hat{\xi}_d^{-1} - \sum_k \mathcal{G}^R(k_+, \mu_+) \times \mathcal{G}^A(k_-, \mu_-) \right]^{-1} \quad (32)$$

with

$$\begin{aligned}\hat{\xi}_d^{-1} &\equiv \frac{v_+}{v_+^2 - v_-^2} \hat{\gamma}_0 \times \hat{\gamma}_0 - \frac{v_-}{v_+^2 - v_-^2} \hat{\gamma}_5 \times \hat{\gamma}_5, \\ \hat{\mathcal{G}}^R(k_+, \mu_+) &\equiv \frac{\mathcal{F}_{0,+}}{\mathcal{F}_{0,+}^2 - k_+^2 - \mathcal{F}_{5,+}^2} \hat{\gamma}_0 - \sum_{j=1}^3 k_{+,j} \hat{\gamma}_j - \frac{\mathcal{F}_{5,+}}{\mathcal{F}_{0,+}^2 - k_+^2 - \mathcal{F}_{5,+}^2} \hat{\gamma}_5, \\ \hat{\mathcal{G}}^A(k_-, \mu_-) &\equiv \frac{\mathcal{F}_{0,-}^*}{(\mathcal{F}_{0,-}^*)^2 - k_-^2 - (\mathcal{F}_{5,-}^*)^2} \hat{\gamma}_0 - \sum_{j=1}^3 k_{-,j} \hat{\gamma}_j - \frac{\mathcal{F}_{5,-}^*}{(\mathcal{F}_{0,-}^*)^2 - k_-^2 - (\mathcal{F}_{5,-}^*)^2} \hat{\gamma}_5, \\ 2v_\pm &\equiv \sqrt{\Delta_s^2 - B^2} \pm 2\pi(\Delta_{0,0} - \Delta_{5,5}).\end{aligned}$$

The subscript on \mathcal{F}_j stands for its ω -dependence; $\mathcal{F}_{j,\pm} \equiv \mathcal{F}_j(\mu \pm \frac{\omega}{2}, m)$, where the μ - and m -dependence of \mathcal{F}_j are determined by the preceding gap equation, eqs. (16-18).

Taking q to be zero, we get a relatively simpler expression for eq. (32),

$$\begin{aligned}\bar{\Gamma}^{\text{dif}}(0, \omega) &= f_1^{-1} \Gamma_1 + f_2^{-1} \Gamma_2 + f_3^{-1} \Gamma_3 + f_4^{-1} \Gamma_4, \\ f_1 &= a_1^2 - \delta a_{04}^2 + \delta a_{23}^2, \quad f_2 = a_1^2 - a_{04}^2 + a_{23}^2, \\ f_3 &= 9a_1^2 - \delta a_{04}^2 + \delta a_{23}^2, \quad f_4 = 9a_1^2 - a_{04}^2 + a_{23}^2,\end{aligned} \quad (33)$$

with $\delta a_{ij} \equiv a_i - a_j$, $a_{ij} \equiv a_i + a_j$ and

$$a_0 \equiv \frac{v_+}{v_+^2 - v_-^2} - \sum_k \frac{\mathcal{F}_{0,+} \mathcal{F}_{0,-}^*}{(k^2 - \mathcal{F}_{0,+}^2 + \mathcal{F}_{5,+}^2)(k^2 - (\mathcal{F}_{0,-}^*)^2 + (\mathcal{F}_{5,-}^*)^2)}, \quad (34)$$

$$a_1 \equiv - \sum_k \frac{k_x^2}{(k^2 - \mathcal{F}_{0,+}^2 + \mathcal{F}_{5,+}^2)(k^2 - (\mathcal{F}_{0,-}^*)^2 + (\mathcal{F}_{5,-}^*)^2)}, \quad (35)$$

$$a_2 \equiv \sum_k \frac{\mathcal{F}_{0,+} \mathcal{F}_{5,-}^*}{(k^2 - \mathcal{F}_{0,+}^2 + \mathcal{F}_{5,+}^2)(k^2 - (\mathcal{F}_{0,-}^*)^2 + (\mathcal{F}_{5,-}^*)^2)}, \quad (36)$$

$$a_3 \equiv \sum_k \frac{\mathcal{F}_{5,+} \mathcal{F}_{0,-}^*}{(k^2 - \mathcal{F}_{0,+}^2 + \mathcal{F}_{5,+}^2)(k^2 - (\mathcal{F}_{0,-}^*)^2 + (\mathcal{F}_{5,-}^*)^2)}, \quad (37)$$

$$a_4 \equiv - \frac{v_-}{v_+^2 - v_-^2} - \sum_k \frac{\mathcal{F}_{5,+} \mathcal{F}_{5,-}^*}{(k^2 - \mathcal{F}_{0,+}^2 + \mathcal{F}_{5,+}^2)(k^2 - (\mathcal{F}_{0,-}^*)^2 + (\mathcal{F}_{5,-}^*)^2)}, \quad (38)$$

Four Γ_j in eq. (33) turns out to be all regular functions (tensors) of ω [11]. The only possibility is, therefore, the diffusion pole appears in one of the four coefficients f_j . In fact, employing the same technique invented in Ref. [11], we can easily show that eq. (16) requires f_4 to be zero at $\omega = 0$. The other three coefficients are generally truncated by some finite infrared cutoff. Each cutoff stands for (the inverse of) the relaxation time of a certain internal degree of freedom other than charge density.

When the topological-mass-type disorder is absent [11], f_3 also exhibits the diffusive behaviour at the massless point, $m = 0$. This is because, in the presence of only the γ_0 -type disorder potential, $\hat{\gamma}_{45}$ always commutes with a hamiltonian at the TQCP, so that not only the charge density but the corresponding parity density \P also follow a diffusion equation. Indeed, when substituted into eq. (30), $f_3^{-1}\Gamma_3$ contributes to the correlation function of this parity density, while $f_4^{-1}\Gamma_4$ does to that of the charge density. When their advanced lines are time-reversed as in eq. (31), both Γ_3 and Γ_4 result in the same magnitude of the positive weak-localization (AWL) correction to the charge conductivity. Thus, the additional $U(1)$ symmetry recovery at the TQCP induces the ‘doubling phenomena’ of the quantum conductivity correction around this massless point.

In the presence of the topological-mass-type disorder, however, the relaxation time of this parity density, given below, *always remains finite* in the *whole* μ - m parameter space,

$$\tau_{\text{topo}}^{-1} \equiv \left\{ \frac{\partial f_4}{\partial \omega} (f_3 - f_4) \right\}_{|\omega=0} = \left\{ \frac{\partial f_4}{\partial \omega} (-a_0 a_4 + a_2 a_3) \right\}_{|\omega=0}. \quad (39)$$

Namely, though both a_2 and a_3 in the r.h.s. vanish at $\psi_2 \equiv -\mu \sinh \theta + m \cosh \theta = 0$, a_4 never vanishes even at $\psi_2 = 0$, due to the first term in eq. (38), $-\frac{v_-}{v_+^2 - v_-^2}$. Indeed, once the γ_5 -type impurity potential is introduced, the parity density is generally a non-conserved quantity. As a result, unlike in Ref. [11], only the charge diffusion pole results in the positive weak-localization correction, while that of the parity diffusion mode remains always ‘gapped’ in the entire μ - m parameter space.

6. summary

From the bulk-edge correspondence, the topological quantum critical point (TQCP) which intervenes the three-dimensional topological insulator and an ordinary insulator is expected to be stable against any non-magnetic disorders, provided that each surface state supported in the topological insulator phase is stable against the same perturbations. To understand the stability of this 3-d TQCP, we first employ the ‘Berry phase’ argument and show that any backward scattering process which conserves the parity density degree of freedom, $\psi^\dagger \gamma_{45} \psi$, is always set off by its \mathcal{T} -reversal counter-process. This observation upholds more directly our previous surmise in Ref [11], where two of the authors conjectured that, when the system transits from the topological

\P $\hat{\gamma}_{45}$ is spatially-inversion odd, while time-reversal even, so that we call the corresponding density, $\psi^\dagger \hat{\gamma}_{45} \psi$, as the parity density.

insulator side to the ordinary insulator side, the parity density always becomes a conserved quantity once. However, it is still an open issue *how* the parity density becomes a conserved quantity at these transition points (or regions) *in the presence of generic non-magnetic disorders*. Namely, the ‘Berry phase’ argument *only* confirms that, as far as the parity density is a conserved quantity, the 3-d TQCP remains delocalized (or critical) even in the presence of sufficiently strong generic non-magnetic disorders.

In fact, as for those backward scattering processes which do not conserve the parity density, the above ‘Berry phase’ argument does not work at all. To understand these generic \mathcal{T} -symmetric situations, we further derive the self-consistent Born phase diagram in the presence of general non-magnetic disorders. We found that the derived scB phase diagram is basically same as that in the case with only the chemical-potential-type disorder. Namely, as in Ref. [11], there exists a certain critical disorder strength, below which the two gapped phases (the topological insulator and an ordinary insulator) are always separated by the *direct* quantum phase transition point in the μ - m parameter space. When the disorder strength exceeds this critical value, this direct transition point becomes a *finite region* of the diffusive metallic phase.

As for the quantum conductivity correction, the situation changes drastically. On increasing the topological-mass type disorder potential, we found that the diffusive parity density mode observed at the 3-d TQCP always acquires a *finite relaxation time* in the *entire* μ - m parameter space. This indicates that the ‘doubling phenomena’ of the quantum conductivity correction previously observed at the TQCP [11] becomes suppressed in the presence of γ_5 -type disorder potential.

7. Acknowledgments

RS and RN were supported by the Institute of Physical and Chemical Research (RIKEN) and SM was supported by Grants-in-Aid for Scientific Research from the Ministry of Education, Culture, Sports, Science and Technology (MEXT) of Japan.

References

- [1] J. E. Moore and L. Balents, Phys. Rev. B **75**, 121306 (R) (2007).
- [2] R. Roy, Phys. Rev. B **79**, 195322 (2009).
- [3] L. Fu, C. L. Kane and E. J. Mele, Phys. Rev. Lett. **98**, 106803 (2007); Phys. Rev. B **76**, 045302 (2007).
- [4] C. L. Kane and E. J. Mele, Phys. Rev. Lett. **95**, 146802 (2005).
- [5] C. Wu, B. A. Bernevig and S.-C. Zhang, Phys. Rev. Lett. **96**, 106401 (2006).
- [6] C. Xu and J. E. Moore, Phys. Rev. B **73**, 045322 (2006).
- [7] S. Murakami, New J. Phys. **9**, 356 (2007); Errata **10**, 029802 (2008).
- [8] S. Murakami and S. Kuga, Phys. Rev. B **78**, 165313 (2008).
- [9] X. L. Qi, T. L. Hughes and S. C. Zhang, Phys. Rev. B **78**, 195424 (2008).
- [10] A. P. Schnyder, S. Ryu, A. Furusaki, and A. W. W. Ludwig, Phys. Rev. B **78**, 195125 (2008).
- [11] R. Shindou and S. Murakami, Phys. Rev. B **79**, 045321 (2009).
- [12] J. H. Bardarson, J. Tworzydło, P. W. Brouwer and C. W. J. Beenakker, Phys. Rev. Lett. **99**, 106801 (2007).

- [13] S. Ryu, C. Mudry, H. Obuse, and A. Furusaki, Phys. Rev. Lett. **99**, 116601 (2007).
- [14] K. Nomura, M. Koshino, S. Ryu, Phys. Rev. Lett. **99**, 146806 (2007).
- [15] E. Abrahams, P. W. Anderson, D. C. Licciardello and T. V. Ramakrishnan, Phys. Rev. Lett. **42**, 673 (1979).
- [16] B. I. Halperin, Phys. Rev. B **25**, 2185 (1982).
- [17] H. Aoki and T. Ando, Phys. Rev. Lett. **54**, 831 (1985).
- [18] Y. Huo and R. N. Bhatt, Phys. Rev. Lett **68**, 1375 (1992)
- [19] M. Onoda, Y. Avishai and N. Nagaosa, Phys. Rev. Lett. **98**, 076802 (2007).
- [20] H. Obuse, A. Furusaki, S. Ryu and C. Mudry, Phys. Rev. B **76**, 075301 (2007).
- [21] C. W. Groth, M. Wimmer, A. R. Akhmerov, J. Tworzydlo and C. W. J. Beenakker, Phys. Rev. Lett. **103**, 196805 (2009).
- [22] T. Ando and T. Nakanishi, J. Phys. Soc. Jpn. **67**, 1704 (1998); T. Ando, T. Nakanishi and R. Saito, J. Phys. Soc. Jpn. **67**, 2857 (1998).
- [23] T. Ando and H. Suzuura, J. Phys. Soc. Jpn. **71**, 2753 (2002); H. Suzuura and T. Ando, Phys. Rev. Lett, **89**, 266603 (2002).
- [24] D. Hsieh, et al. Nature **452**, 970 (2008).
- [25] Y. L. Chen, et al. Science **325**, 178 (2009).
- [26] H. J. Zhang, et al. Nature Physics **5**, 438 (2009)
- [27] D. Hsieh, et al. Science **323**, 919 (2009).
- [28] D. Hsieh, et al. Nature **460**, 1101 (2009).